

Geophysical Research Letters®



RESEARCH LETTER

10.1029/2024GL111391

Special Collection:

Land-atmosphere coupling:
measurement, modelling and
analysis

Key Points:

- The trend of gross primary productivity in China's drylands has shown a marked increase, especially after 2011
- The leaf area index serves as a crucial intermediary in modulating the indirect effects of climatic factors on gross primary productivity
- The complex interactions between climatic factors and the leaf area index on gross primary productivity vary along the aridity gradient

Supporting Information:

Supporting Information may be found in the online version of this article.

Correspondence to:

X. Wang and T. Cheng,
wangxyfd@fudan.edu.cn;
ttcheng@fudan.edu.cn

Citation:

Gong, H., Wang, G., Wang, X., Kuang, Z., & Cheng, T. (2024). Trajectories of terrestrial vegetation productivity and its driving factors in China's drylands. *Geophysical Research Letters*, 51, e2024GL111391. <https://doi.org/10.1029/2024GL111391>

Received 18 JUL 2024

Accepted 3 OCT 2024

Trajectories of Terrestrial Vegetation Productivity and Its Driving Factors in China's Drylands

Haixing Gong^{1,2} , Guoyin Wang^{1,3,4} , Xiaoyan Wang^{1,3,5,6} , Zexing Kuang⁷, and Tiantao Cheng^{1,3,4} 

¹Department of Atmospheric and Oceanic Sciences & Institute of Atmospheric Sciences, Fudan University, Shanghai, China, ²Key Laboratory of Polar Atmosphere-ocean-ice System for Weather and Climate, Ministry of Education, Fudan University, Shanghai, China, ³Shanghai Key Laboratory of Ocean-land-atmosphere Boundary Dynamics and Climate Change, Fudan University, Shanghai, China, ⁴Shanghai Frontiers Science Center of Atmosphere-Ocean Interaction, Shanghai, China, ⁵CMA-FDU Joint Laboratory of Marine Meteorology, Shanghai, China, ⁶Shanghai Institute of Pollution Control and Ecological Security, Shanghai, China, ⁷Department of Environmental Science and Engineering, Fudan University, Shanghai, China

Abstract Climate change and large-scale ecological restoration programs have profoundly influenced vegetation greening and gross primary productivity (GPP) in China's drylands. However, the specific pathways through which climatic factors and vegetation greening influence GPP remain poorly understood. This study examines the spatiotemporal changes in GPP across China's drylands from 2001 to 2020 and investigates the direct and indirect effects of climatic factors and leaf area index (LAI) on GPP. The results reveal that the overall improvement in vegetation cover has positively increased GPP in these regions. Although the direct effects of climatic factors on GPP are minimal, they exert a substantial indirect effect by regulating vegetation growth, highlighting that LAI is a key intermediary in mediating the effects of climatic factors on GPP. Furthermore, these complex interactions vary significantly along the aridity gradient. This study emphasizes the necessity of comprehensively considering the intricate interactions among multiple climate and vegetation factors.

Plain Language Summary China's drylands have undergone significant vegetation greening and ecological restoration, characterized by transitions toward forests, grasslands, and croplands. These changes have greatly enhanced gross primary productivity (GPP), a key indicator of ecosystem health and functionality. This study reveals that the increase in GPP results from the combined effects of climate change and improved vegetation cover. Although climatic factors like temperature, precipitation, and solar radiation directly affect GPP to a lesser extent, they indirectly boost it by altering vegetation growth conditions. Among the various factors, the increase in vegetation cover has the most direct and substantial positive effect on GPP, especially in semi-arid and dry sub-humid regions, where ecological restoration efforts are concentrated. Furthermore, the study indicates that the center of gravity for vegetation productivity in China's drylands is gradually shifting westward, and predicts that most areas will maintain the current trend of increasing vegetation productivity. Overall, under the dual impetus of climate change and greening initiatives, the vegetation in China's drylands has exhibited strong vitality. This not only benefits ecological environment improvement but also supports climate change mitigation and contributes to carbon peaking and carbon neutrality goals.

1. Introduction

China possesses the world's largest drylands, supporting over 38% of its population (Huang et al., 2017; Li et al., 2021). These regions are ecologically fragile and highly susceptible to climate change and human activities (Zhou et al., 2016). The continuous expansion of drylands and increased desertification pose significant threats to the local environment (Li et al., 2015). To mitigate these issues, the Chinese government has implemented a series of ecological restoration programs since the late twentieth century, such as the Three-North Shelter Forest Program and the Beijing-Tianjin Sand Source Control Project (Lu et al., 2018; Wang et al., 2023). These initiatives aim to enhance the ecological environment by altering land use patterns and promoting artificial vegetation restoration (Wu et al., 2024). Despite these efforts, the effectiveness and impact of vegetation restoration in drylands remain subjects of debate, especially in the context of ongoing climate change (Wang et al., 2023; Wu et al., 2024; Xu et al., 2023). Consequently, in-depth research on the dynamics of vegetation in China's drylands is essential for a comprehensive understanding of both regional and global environmental changes.

© 2024. The Author(s).

This is an open access article under the terms of the [Creative Commons Attribution-NonCommercial-NoDerivs License](#), which permits use and distribution in any medium, provided the original work is properly cited, the use is non-commercial and no modifications or adaptations are made.

Numerous studies have demonstrated a significant greening trend in China by monitoring spatiotemporal variations in vegetation indices, such as the normalized difference vegetation index (NDVI) and leaf area index (LAI) (Chen et al., 2019; Piao et al., 2020; Xu et al., 2023). Nevertheless, despite their ability to represent vegetation cover and growth status, these indices have limitations in fully assessing the sustainability and carrying capacity of dryland ecosystems (Hu et al., 2022; Zhang et al., 2023). Gross primary productivity (GPP), a core indicator of ecosystem carbon cycling and energy flow (Chen, Feng, et al., 2021), is essential for evaluating the effectiveness of ecological restoration and the adaptability of ecosystems to climate change (Ren et al., 2024). Although global studies provide a macro perspective on the spatiotemporal variations of GPP in drylands, their typically coarse spatial resolution (typically 0.25°) often fails to accurately capture the subtle variations in GPP caused by microclimate changes and land use differences, especially in the complex terrains with delicate ecological gradients across China's drylands (Wang et al., 2022; Yao et al., 2020). Given the vast expanse of China's drylands (Li et al., 2021), even minor changes in carbon effects per unit area can cumulatively have a significant impact on the global carbon cycle and climate system (Ahlström et al., 2015). Therefore, there is a pressing need for detailed investigations into the spatiotemporal patterns (including trends, fluctuations, and abrupt changes) and future trajectories of GPP in these regions.

Climate change plays a pivotal role in regulating GPP dynamics. Previous research has amply demonstrated that temperature, precipitation, and solar radiation directly affect the physiological activities and growth cycles of vegetation, thereby influencing ecosystem carbon sequestration (Chen et al., 2021a, 2021b). These studies have thoroughly explored the direct mechanisms by which climatic factors influence GPP, laying a crucial foundation for understanding the impacts of climate change on ecosystems. However, it is important to note that many studies have not adequately revealed the mediating role of vegetation indices, such as LAI, between climatic factors and GPP (Yao et al., 2020; Yu et al., 2013). LAI, a key parameter describing the structure of the vegetation canopy (Yan et al., 2019), not only reflects the quantity and distribution of plant leaves but also indirectly regulates ecosystem changes by influencing vegetation responses to climatic factors (Bonan, 2008; Deng, Wang, Bai, Luo, Wu, Chen, & et al., 2020). This regulatory role has the potential to mitigate or even reverse the anticipated impacts of climatic factors (Xu et al., 2023). Therefore, ignoring the mediating role of LAI may partially obscure the true extent of the climatic factors' impact on GPP. Xie et al. (2020) utilized ridge regression to quantify the contributions of climate change and LAI to GPP changes in the Three-North region. However, this approach primarily focused on the direct effects, potentially underestimating the true contribution of climatic factors. This underestimation largely stems from insufficient consideration of indirect effects mediated through vegetation indices such as LAI. Although previous studies have documented significant greening trends in China's drylands (Fan et al., 2024; Li et al., 2021), current research frameworks frequently fail to comprehensively integrate climate and vegetation elements to explore their pathways of influence on GPP (Xie et al., 2019; Yu et al., 2013). This further underscores the urgency of investigating the interactions between climate and vegetation. Specifically, the intricate mechanisms through which climatic factors indirectly affect GPP via LAI, and how vegetation changes feedback into the climate system to influence GPP, require systematic investigation and deeper understanding. Consequently, further research is needed to more effectively focus on climate-vegetation interactions, and to delve deeper into their combined pathways of influence on GPP.

This study aims to: (a) identify the evolving patterns of climatic factors, land use, and vegetation cover in China's drylands from 2001 to 2020; (b) delve deeply into the intricate spatiotemporal variations in GPP, focusing on trends, fluctuations, abrupt changes, and future sustainability; (c) systematically evaluate the direct and indirect pathways through which climate change and vegetation greening affect GPP changes. These findings will provide crucial insights for ecological management in China's drylands and similar regions worldwide.

2. Materials and Methods

2.1. Study Area

This study focuses on China's drylands, defined as regions where the ratio of average annual precipitation to potential evapotranspiration is less than 0.65 (Huang et al., 2016). These regions are mainly located in North China, Northwest China, and Southwest China (Figure S1 in Supporting Information S1). Due to the combined effects of continental climate, Asian monsoon, and the Qinghai-Tibet Plateau, the climate characteristics of these drylands exhibit significant spatial heterogeneity, gradually transitioning from relatively warm and humid dry sub-humid regions to hot and dry hyper-arid regions. Furthermore, the environmental conditions in China's

drylands display diverse trends, including a slowdown in warming ($0.01^{\circ}\text{C}\cdot\text{yr}^{-1}$, $P = 0.39$), a significant rise in precipitation ($1.56\text{ mm}\cdot\text{yr}^{-1}$, $P < 0.05$), and a notable decrease in solar radiation ($-0.23\text{ W}\cdot\text{m}^{-2}\text{ yr}^{-1}$, $P < 0.01$) (Figure S2 in Supporting Information S1).

2.2. Data and Methods

The study utilized land use data (MCD12Q1, PFT classification) and gross primary productivity (GPP, MOD17A2H) data provided by the Moderate Resolution Imaging Spectroradiometer (MODIS) of the National Aeronautics and Space Administration (NASA) from 2001 to 2020. These data sets have temporal resolutions of annual and 8-day intervals, respectively, and a spatial resolution of 500 m (Friedl & Sulla-Menashe, 2019; Running et al., 2015). To analyze the driving factors of GPP changes, major climatic factors and vegetation indices were included, including temperature, precipitation, solar radiation, and leaf area index (LAI) (Chen, Feng, et al., 2021). Specifically, monthly average temperature and monthly total precipitation data were sourced from the 1 km China temperature and precipitation data sets published by Peng et al. (2019), which have been widely used in China and its drylands (Fu et al., 2024). Solar radiation data were sourced from the Global Land Surface Satellite (GLASS), with a temporal resolution of 3 hr and a spatial resolution of 5 km, validated by Zhang et al. (2014). LAI data were also derived from the GLASS, with a spatial resolution of 250 m and a temporal resolution of 8 days (Xiao et al., 2016). To ensure spatial consistency, land use data were aggregated using the “majority” method, and bilinear interpolation was employed to aggregate GPP, LAI, and climate data to a 4 km grid. Temporally, depending on the data type, we resampled the data to monthly or annual intervals: using the “sum” method for GPP and precipitation, the “maximum value composite” method for LAI, and the “average” method for temperature and radiation. Further details on the data processing methods can be found in Gong et al. (2023).

To further investigate the spatiotemporal characteristics of GPP, this study employed various analytical methods, including empirical orthogonal function (EOF) decomposition, Theil–Sen Median trend analysis, the Mann–Kendall test, the Hurst index, and the shifting center of gravity model. EOF was employed to extract the primary spatial modes by analyzing the spatial covariance structure, with mode independence determined using the North criterion (Preisendorfer & Mobley, 1988). The Theil–Sen median trend analysis, a robust non-parametric statistical method, was employed to evaluate the trends in GPP (Sen, 1968; Theil, 1992). The Mann–Kendall test was used to detect significant trends and abrupt changes in GPP (Libiseller & Grimvall, 2002), and can be combined with the Theil–Sen method to explore long-term trends (Deng, Wang, Bai, Luo, Wu, Cao, & et al., 2020). Furthermore, the Hurst index was applied to quantitatively assess the sustainability of time series (Hurst, 1951), while the shifting center of gravity model focused on the spatial dynamic evolution of GPP to identify its spatial evolution patterns (Balsa-Barreiro et al., 2019). Finally, the path analysis algorithm was used to elucidate the impact pathways of climate and vegetation factors on GPP (Hollar, 2018; Xu et al., 2023). The method decomposes the combined effects into direct and indirect effects, where the direct effect refers to the immediate impact of an environmental variable on GPP, while the indirect effect denotes the influence mediated through other intermediate variables. Although MODIS–GPP is widely used to assess spatiotemporal variations of GPP in global drylands (Verma et al., 2014; Yao et al., 2020), to account for the uncertainties in MODIS–GPP (Huang et al., 2021), this study employed three additional GPP data sets from different sources (Bi et al., 2022; Leng et al., 2024; X. Li & Xiao, 2019) to verify the reliability and robustness of the path analysis results. Detailed descriptions of these data and methods are provided in Texts S1–S7 in Supporting Information S1.

3. Results and Discussion

3.1. Evolving Patterns of Land Use and Vegetation Cover

China's drylands were predominantly composed of barren lands, grasslands, croplands, and forests, with the leaf area index (LAI) being higher in the east and lower in the west. Forests, shrubs, and croplands exhibited relatively high LAI, whereas grasslands demonstrated lower values (Figure S3 in Supporting Information S1). Additionally, approximately 8.3% of China's drylands experienced changes in land use types, primarily among barren lands, grasslands, and croplands, as well as transitions to forests (Figures 1a and 1b). Specifically, croplands and barren lands were mainly converted into forests and grasslands, while a significant proportion of grasslands was

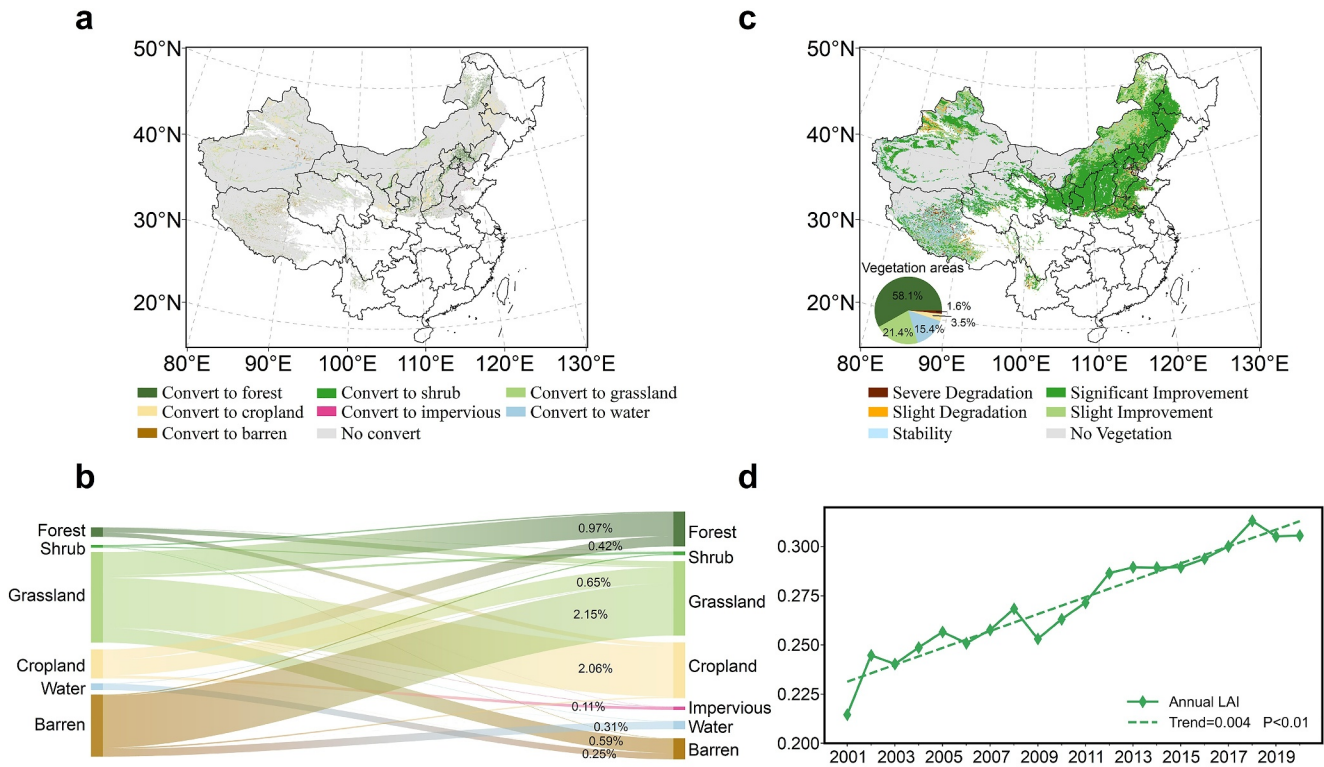


Figure 1. Land use type transitions and annual variations in LAI in China's drylands from 2001 to 2020. (a) The transitions in land use types and (b) the percentage area changes for each land use type. (c) The regions categorized based on Sen_{LAI} , calculated using Theil-Sen method, into stable areas ($-0.0005 < Sen_{LAI} < 0.0005$), improved areas ($Sen_{LAI} \geq 0.0005$), and degraded areas ($Sen_{LAI} \leq -0.0005$). Additionally, at a confidence level of 0.05, the Mann-Kendall test indicates areas of significant change and non-significant change. (d) Annual variations in the average LAI across the entire China's drylands.

transformed into forests or croplands. Overall, due to land use changes, the forest area increased by approximately 1.04%, while the area of barren lands decreased by 1.69%.

Over the past two decades, 37.9% of the regions in China's drylands remained non-vegetated with a LAI of 0 (Figure S3d in Supporting Information S1). Consequently, these non-vegetated areas were excluded from the Theil-Sen median trend analysis and the Mann-Kendall test. Within the remaining vegetated areas, 79.5% showed vegetation improvement, while only 5.1% experienced degradation (Figures 1c and 1d). Significant vegetation improvements were mainly concentrated in southern North China, Northeast China, and parts of northwestern Xinjiang, whereas slight improvements were predominantly seen in northern North China. These improvements are largely attributed to the effective implementation of ecological protection and restoration measures (Lu et al., 2018). Despite these efforts, some regions have experienced vegetation degradation (Figures 1a and 1c), primarily due to desertification trends in parts of the Tibetan Plateau, the conversion of land to barren lands and croplands around the Altai Mountains, and the reduction of natural vegetation in the core areas of the Beijing-Tianjin-Hebei urban agglomeration due to rapid urbanization. These degraded areas not only directly reduce vegetation productivity but also pose a long-term threat to the ecological balance due to their sensitivity to climate change (Ma et al., 2019; Wei et al., 2016).

3.2. Spatiotemporal Characteristics of Gross Primary Productivity

The empirical orthogonal function (EOF) decomposition was applied to the gross primary productivity (GPP), revealing that the first two principal modes accounted for a cumulative variance contribution rate of 72.18%, effectively capturing the primary patterns of GPP variation in China's drylands. Specifically, the first principal mode (EOF1) alone contributed 61.68% to the variance, significantly surpassing the other modes. EOF1 displayed overall positive values, and its temporal coefficient (PC1) exhibited a significant upward trend, indicating an increasing trend of GPP (Figures 2a and 2b). Subsequent analyses, employing the Theil-Sen method and Mann-Kendall test, further confirmed that 63.1% of the vegetated areas experienced a significant GPP increase, and

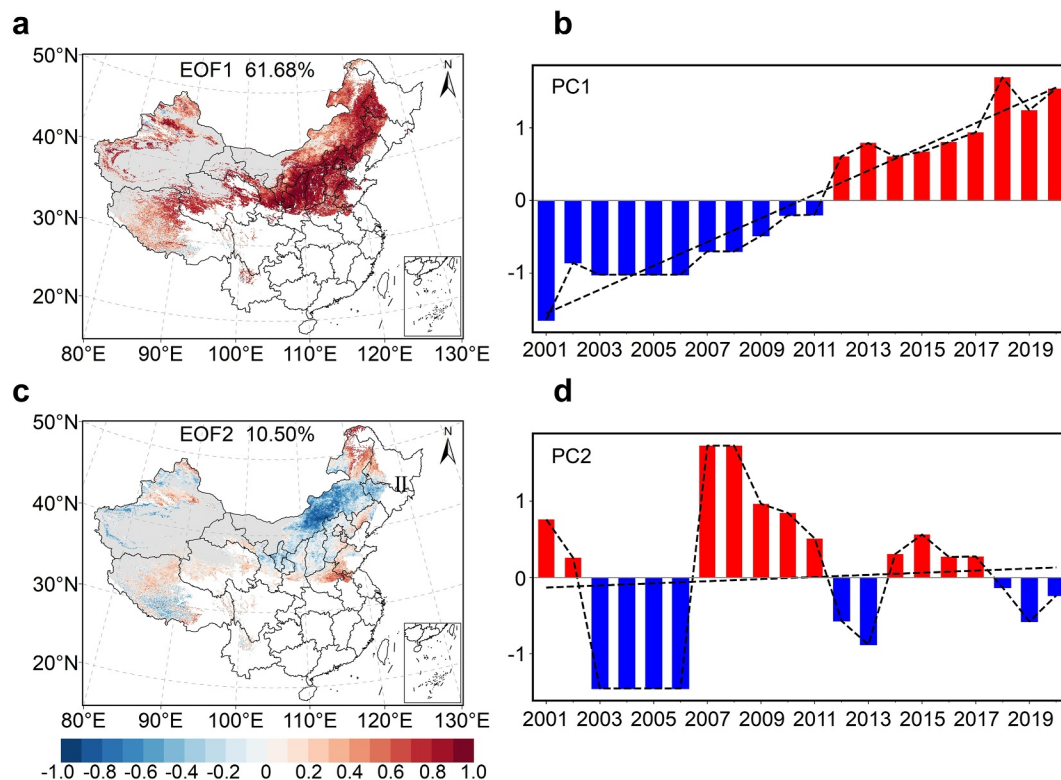


Figure 2. Spatial modes and temporal analysis of GPP in China's drylands from 2001 to 2020. (a–b) Spatial distribution and temporal coefficient of the first principal mode. (c–d) Spatial distribution and temporal coefficient of the second principal mode.

30.7% exhibited a slight increase (Figure 3a). This upward trend aligned with satellite observations indicating enhanced vegetation cover, corroborating the actual enhancement of vegetation productivity in this region (Figure 2c). This positive outcome is strongly associated with China's recent vigorous implementation of ecological restoration programs (Wang et al., 2023). Notably, only 6.1% of the vegetated areas showed a decreasing GPP trend. Moreover, the Hurst index projections suggested an enduring continuation of this positive growth trajectory in 82.4% of the region in the future, primarily located in North China and Northeast China (Figure 3b). However, caution is warranted as 4.1% of the areas may undergo continuous degradation, while future trends in another 13.3% remain uncertain due to complex factors such as climate change, human activities, and adjustments in policies. Interestingly, the shifting center of gravity model revealed a gradual westward migration of the GPP center of gravity from densely vegetated eastern locales to the sparser western territories over the last two decades (Figure 3c), suggesting an overall ecological improvement.

PC1 indicated an accelerated GPP growth since 2011 (Figure 2b), and this trend was statistically validated by the Mann-Kendall test. The test's UF curve exceeded the significance threshold ($U_a = 1.96$) in 2011, signaling a notable GPP increase (Figure S4 in Supporting Information S1). This finding aligns with the results of Chen, Feng, et al. (2021), which identified accelerated growth in China's GPP starting in 2010. Conversely, the second principal mode (EOF2), despite contributing only 10.50% to the variance, still represented a typical pattern of GPP in China's drylands (Figures 2c and 2d). Compared to EOF1, EOF2 exhibited greater spatial heterogeneity, reflecting the spatial unevenness observed in the actual GPP distribution of drylands. EOF1 primarily underscored the general trend of GPP, whereas EOF2 provided a detailed insight into the spatial unevenness and temporal fluctuations of GPP. In summary, while previous studies have significantly advanced our understanding of the GPP growth (Ma et al., 2019; Xie et al., 2020), they have often overlooked aspects such as spatial heterogeneity, abrupt changes, spatial shifts, and future sustainability. This study, utilizing a higher spatiotemporal resolution and multidimensional analytical methods, not only corroborated previous findings but also illuminated new perspectives with important implications for future ecological management.

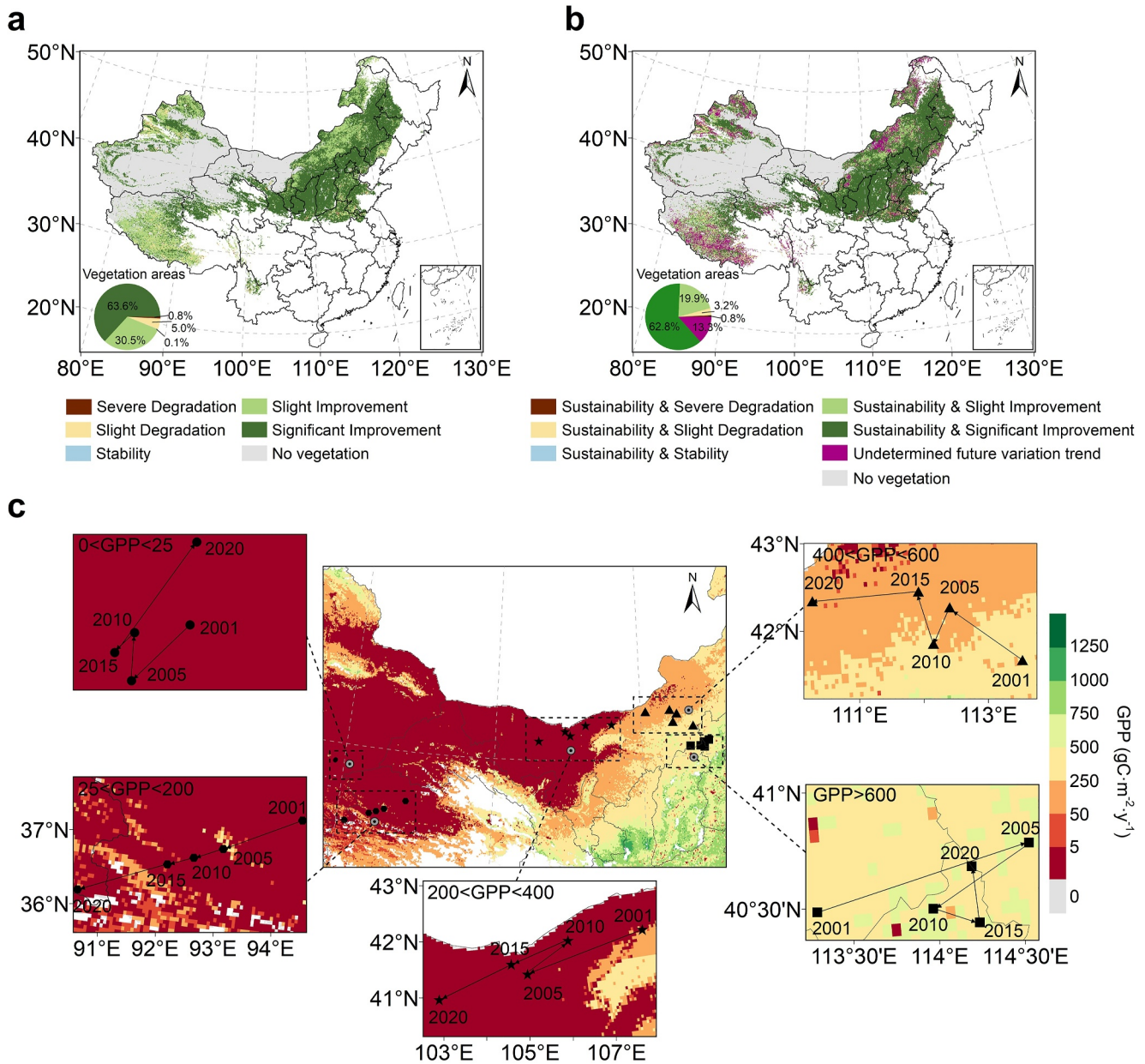


Figure 3. Spatiotemporal evolution characteristics of GPP in China's drylands from 2001 to 2020. (a) Interannual variation trends of GPP based on Theil-Sen median trend analysis and Mann-Kendall test, and (b) the future sustainability of GPP interannual variations further integrating the Hurst index. (c) The shift trajectory of the GPP center of gravity.

3.3. Influencing Pathways of Climate and Vegetation Cover Changes Affecting GPP

This study analyzed the combined impact pathways of climate and vegetation cover changes on GPP using path analysis. In this path model, direct effects represent the immediate impact of an environmental variable on GPP while controlling for other variables. Indirect effects, on the other hand, signify the variable's influence on GPP mediated through other intermediate variables. The direct effects of temperature (T_{mp}), precipitation (Pre), and solar radiation (Rad) on GPP in China's drylands were relatively minor, with influence coefficients of 0.10, 0.15, and 0.14, respectively. These coefficients were significantly lower than the direct impact of LAI on GPP (0.57) (Figure 4a). This is primarily because LAI, as a key indicator of vegetation structure, exerts a substantial direct impact on GPP. However, it is noteworthy that these climatic factors significantly affected GPP indirectly by regulating LAI (T_{mp}→LAI→GPP: 0.47; Pre→LAI→GPP: 0.43; Rad→LAI→GPP: 0.35) (Figure 4b). Taking the

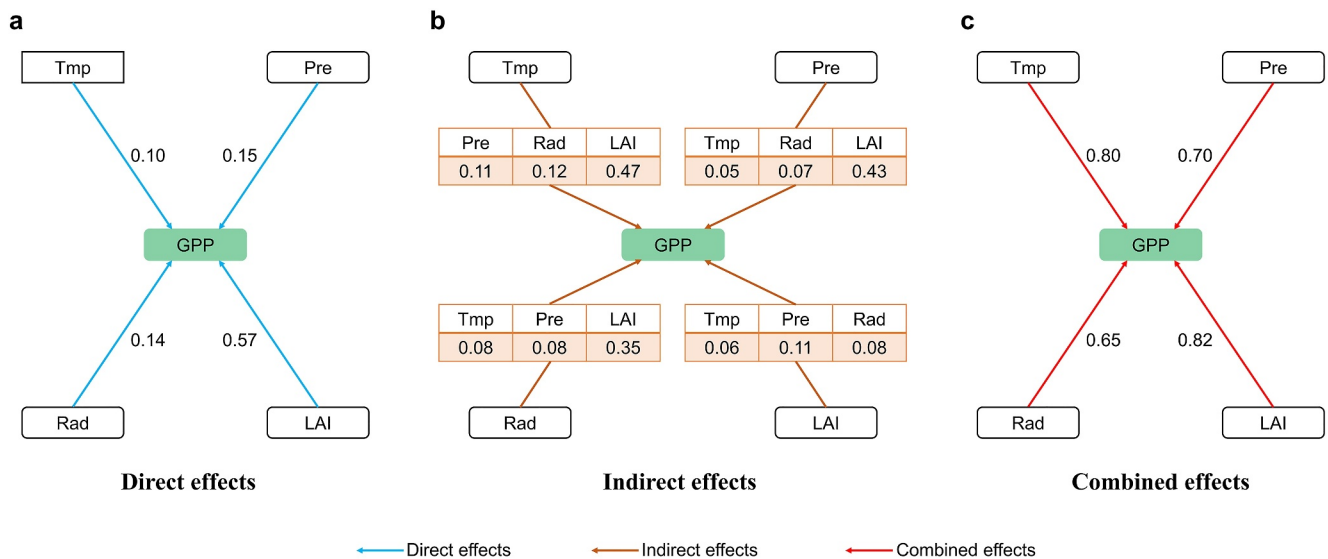


Figure 4. The (a) direct, (b) indirect, and (c) combined effects of climatic factors (temperature, precipitation, solar radiation) and vegetation cover (LAI) on GPP in China's drylands from 2001 to 2020.

pathway Pre→LAI→GPP as an example, since water is an important stressor in drylands (Gong et al., 2024), the increase in precipitation enhances vegetation growth and greening, thereby indirectly boosting vegetation productivity. This highlights that although the direct effects of climatic factors on GPP were minor, their indirect effects, mediated through LAI, were substantial, emphasizing LAI's critical role as an intermediary in these processes. Consequently, the combined direct and indirect effects of climatic factors on GPP were substantial (Tmp: 0.80; Pre: 0.70; Rad: 0.65) (Figure 4c). Compared to the ridge regression method that only considers direct effects (Xie et al., 2020), this path analysis provides a more comprehensive assessment of the true contributions of climatic factors. Furthermore, LAI not only had a pronounced direct impact on GPP but also exerted indirect effects through feedback mechanisms (LAI→Tmp→GPP: 0.06; LAI→Pre→GPP: 0.11; LAI→Rad→GPP: 0.08). Similarly, considering the pathway LAI→Pre→GPP, vegetation greening promotes surface evapotranspiration, and the dissipated water vapor further participates in local-scale water recycling, replenishing surface water through precipitation (Cui et al., 2022), thereby indirectly influencing GPP. This complex feedback mechanism is primarily attributed to the regulatory function of vegetation itself: as vegetation cover increases, it can influence local climate conditions (Duveiller et al., 2018; Ge et al., 2023), thereby indirectly affecting GPP. Not only that, climate changes, in turn, generate positive feedback on vegetation growth, further promoting the growth of vegetation (Fan et al., 2024). Moreover, the same analysis was conducted using three additional GPP data sets, yielding consistent results (Figure S5 in Supporting Information S1).

The combined impact, as the sum of direct and indirect effects, reflects the overall effects of environmental variables. When comparing the combined effects of various factors, GPP in China's drylands was predominantly influenced by LAI, followed by temperature, precipitation, and solar radiation (LAI > Tmp > Pre > Rad; Figure 4c). This pattern aligned with the consistency observed between changes in vegetation cover and GPP trends derived from satellite observations. Furthermore, the impact of climate and vegetation cover changes on GPP varied across different aridity gradients (Figure S6 in Supporting Information S1). Specifically, in hyper-arid and arid regions, temperature had the most significant effect on GPP (Tmp > LAI > Rad > Pre) (Figure 4c). This is primarily attributed to the vegetation's distribution predominantly along the fringes of hyper-arid regions (adjacent to arid or semi-arid regions) and across extensive arid regions (Figure S7 in Supporting Information S1). Even during the hot summer, the average temperature in these vegetated areas (approximately 20.8°C) closely approximates the global optimal photosynthesis threshold (around 23°C) (Huang et al., 2019; Wang et al., 2024). Coupled with the high drought tolerance of vegetation (Abel et al., 2023), this makes temperature a pivotal factor influencing GPP. Conversely, in semi-arid and dry sub-humid regions, LAI emerged as the primary driver (LAI > Tmp > Pre > Rad). Notably, in dry sub-humid regions, LAI exerted the most substantial positive effect (0.88), whereas this impact was least pronounced in hyper-arid regions (0.68). This phenomenon can largely be

attributed to the effective enhancement of vegetation cover in semi-arid and dry sub-humid regions, which are focal areas of ecological engineering greening initiatives, while the greening process in hyper-arid regions has been relatively lagging (Xu et al., 2023). This pattern of influence clearly demonstrates that, despite the varying climatic and ecological conditions across different regions, changes in vegetation cover play a crucial role in driving GPP growth, particularly in the relatively wetter arid areas where this effect is more pronounced. Many previous studies analyzed GPP drivers at larger scales, without fully revealing the disparities in vegetation responses across different aridity gradients (Wang et al., 2022), thus somewhat obscuring the nuanced regional differences. However, in the context of changes in China's drylands (Li et al., 2021), more refined multi-scale analyses can offer a comprehensive understanding of dryland heterogeneity and precise interpretations of GPP dynamics.

4. Conclusions

This study examines the spatiotemporal patterns of GPP in China's drylands and the complex relationships among GPP, land use, vegetation cover, and climatic factors. Using various statistical methods, the study reveals that China's drylands have undergone significant land use changes, primarily involving the large-scale conversion of barren lands and grasslands into forests, grasslands, and croplands. These changes have notably increased vegetation cover and GPP, with a marked upward trend since 2011. Additionally, climatic factors and vegetation cover jointly affect GPP through both direct and indirect pathways. Although climatic factors have a relatively modest direct impact on GPP, they significantly influence GPP indirectly by regulating LAI. This not only accurately assesses the true contribution of climatic factors but also underscores LAI's crucial role as a key intermediary linking climate to ecological functions. Notably, the influence of climate and vegetation cover changes on GPP exhibits significant regional heterogeneity across different aridity gradients. In hyper-arid and arid regions, temperature has the most significant combined impact on GPP. Conversely, in semi-arid and dry sub-humid areas, LAI is more influential. These findings suggest that future research should adopt a more integrated approach, considering the interactions between climate and vegetation, to deeply explore their combined pathways of influence on GPP.

However, this study still has several uncertainties. First, the quality of remote sensing data may influence the results. Issues such as cloud cover, sensor errors, and data processing methods can introduce uncertainties. Future research should enhance the quality and reliability of data through multi-source data fusion and improved data processing algorithms. Second, this study primarily examines the impacts of three key climatic factors—temperature, precipitation, and solar radiation—alongside the influence of LAI, a vegetation structural index, on GPP. However, other climatic factors, such as wind speed, soil moisture, and carbon dioxide, as well as physiological aspects of vegetation, like light use efficiency, water use efficiency, and stomatal conductance, also affect vegetation productivity. Future research should incorporate more climatic variables and vegetation physiological parameters to comprehensively assess the mechanisms through which climate change impacts GPP. Lastly, this study does not fully consider the role of human activities, which significantly influence vegetation cover in China's drylands and may further affect GPP. This aspect will be taken into account in our future research.

Data Availability Statement

The land cover data and GPP data are accessible at Friedl and Sulla-Menashe (2019) and Running et al. (2015), respectively. Potential evapotranspiration, temperature and precipitation are accessible at Peng (2024a, 2024b) and Peng (2024c), respectively. Solar radiation and leaf area index products can be obtained from <http://www.glass.umd.edu/DSR/> and <http://www.glass.umd.edu/LAI/MODIS/0.25D/>, respectively. All figures were created using Matplotlib version 3.5.2 (Caswell et al., 2022), available under the Matplotlib license at <https://matplotlib.org/>. Moreover, statistical analyses were conducted on the Python platform (<https://www.python.org/>).

References

- Abel, C., Abdi, A. M., Tagesson, T., Horion, S., & Fensholt, R. (2023). Contrasting ecosystem vegetation response in global drylands under drying and wetting conditions. *Global Change Biology*, 29(14), 3954–3969. <https://doi.org/10.1111/gcb.16745>
- Ahlström, A., Raupach, M. R., Schurgers, G., Smith, B., Armeth, A., Jung, M., et al. (2015). The dominant role of semi-arid ecosystems in the trend and variability of the land CO₂ sink. *Science*, 348(6237), 895–899. <https://doi.org/10.1126/science.aaa1668>
- Balsa-Barreiro, J., Li, Y., Morales, A., & Pentland, A. S. (2019). Globalization and the shifting centers of gravity of world's human dynamics: Implications for sustainability. *Journal of Cleaner Production*, 239, 117923. <https://doi.org/10.1016/j.jclepro.2019.117923>
- Bi, W., He, W., Zhou, Y., Ju, W., Liu, Y., Liu, Y., et al. (2022). A global 0.05° dataset for gross primary production of sunlit and shaded vegetation canopies from 1992 to 2020. *Scientific Data*, 9(1), 213. <https://doi.org/10.1038/s41597-022-01309-2>

Acknowledgments

This work was jointly supported by the National Natural Science Foundation of China (41975075, 42175179, 42075058, 42375183, 41775129) and the Natural Science Foundation of Shanghai (22ZR1404000).

- Bonan, G. B. (2008). Forests and climate change: Forcings, feedbacks, and the climate benefits of forests. *Science*, 320(5882), 1444–1449. <https://doi.org/10.1126/science.1155121>
- Caswell, T., Droettboom, M., Lee, A., Hunter, J., Firing, E., Stansby, D., et al. (2022). Matplotlib v3.5.2 [Software]. *Zenodo*. <https://doi.org/10.5281/zenodo.6513224>
- Chen, C., Park, T., Wang, X., Piao, S., Xu, B., Chaturvedi, R. K., et al. (2019). China and India lead in greening of the world through land-use management. *Nature Sustainability*, 2(2), 122–129. <https://doi.org/10.1038/s41893-019-0220-7>
- Chen, S., Zhang, Y., Wu, Q., Liu, S., Song, C., Xiao, J., et al. (2021). Vegetation structural change and CO₂ fertilization more than offset gross primary production decline caused by reduced solar radiation in China. *Agricultural and Forest Meteorology*, 296, 108207. <https://doi.org/10.1016/j.agrformet.2020.108207>
- Chen, Y., Feng, X., Tian, H., Wu, X., Gao, Z., Feng, Y., et al. (2021). Accelerated increase in vegetation carbon sequestration in China after 2010: A turning point resulting from climate and human interaction. *Global Change Biology*, 27(22), 5848–5864. <https://doi.org/10.1111/gcb.15854>
- Cui, J., Lian, X., Huntingford, C., Gimeno, L., Wang, T., Ding, J., et al. (2022). Global water availability boosted by vegetation-driven changes in atmospheric moisture transport. *Nature Geoscience*, 15(12), 982–988. <https://doi.org/10.1038/s41561-022-01061-7>
- Deng, Y., Wang, S., Bai, X., Luo, G., Wu, L., Cao, Y., et al. (2020). Variation trend of global soil moisture and its cause analysis. *Ecological Indicators*, 110, 105939. <https://doi.org/10.1016/j.ecolind.2019.105939>
- Deng, Y., Wang, S., Bai, X., Luo, G., Wu, L., Chen, F., et al. (2020). Vegetation greening intensified soil drying in some semi-arid and arid areas of the world. *Agricultural and Forest Meteorology*, 292–293, 108103. <https://doi.org/10.1016/j.agrformet.2020.108103>
- Duveiller, G., Hooker, J., & Cescatti, A. (2018). The mark of vegetation change on Earth's surface energy balance. *Nature Communications*, 9(1), 679. <https://doi.org/10.1038/s41467-017-02810-8>
- Fan, X., Qu, Y., Zhang, J., & Bai, E. (2024). China's vegetation restoration programs accelerated vegetation greening on the Loess Plateau. *Agricultural and Forest Meteorology*, 350, 109994. <https://doi.org/10.1016/j.agrformet.2024.109994>
- Friedl, M., & Sulla-Menashe, D. (2019). MCD12Q1 MODIS/Terra+Aqua land cover type yearly L3 global 500m SIN grid V006 [Dataset]. *NASA LP DAAC*. <https://doi.org/10.5067/MODIS/MCD12Q1.006>
- Fu, F., Wang, S., Wu, X., Wei, F., Chen, P., & Gruenzweig, J. M. (2024). Locating hydrologically unsustainable areas for supporting ecological restoration in China's drylands. *Earth's Future*, 12(3). <https://doi.org/10.1029/2023EF004216>
- Ge, J., Huang, X., Zan, B., Qiu, B., Cao, Y., & Guo, W. (2023). Local surface cooling from afforestation amplified by lower aerosol pollution. *Nature Geoscience*, 16(9), 781–788. <https://doi.org/10.1038/s41561-023-01251-x>
- Gong, H., Wang, G., Fan, C., Zhuo, X., Sha, L., Kuang, Z., et al. (2024). Temporal accumulation and lag effects of precipitation on carbon fluxes in terrestrial ecosystems across semi-arid regions in China. *Agricultural and Forest Meteorology*, 356, 110189. <https://doi.org/10.1016/j.agrformet.2024.110189>
- Gong, H., Wang, Y., Wang, G., Gao, Y., Li, G., Kuang, Z., et al. (2023). Quantifying the spatial representativeness of carbon flux footprints of a grassland ecosystem in the semi-arid region. *Journal of Geophysical Research: Atmospheres*, 128(7). <https://doi.org/10.1029/2022JD038269>
- Hollar, D. W. (2018). The method of path coefficients. In D. W. Hollar (Ed.), *Trajectory analysis in health care* (pp. 49–72). Springer International Publishing. https://doi.org/10.1007/978-3-319-59626-6_5
- Hu, Z., Piao, S., Knapp, A. K., Wang, X., Peng, S., Yuan, W., et al. (2022). Decoupling of greenness and gross primary productivity as aridity decreases. *Remote Sensing of Environment*, 279, 113120. <https://doi.org/10.1016/j.rse.2022.113120>
- Huang, J., Ji, M., Xie, Y., Wang, S., He, Y., & Ran, J. (2016). Global semi-arid climate change over last 60 years. *Climate Dynamics*, 46(3), 1131–1150. <https://doi.org/10.1007/s00382-015-2636-8>
- Huang, J., Li, Y., Fu, C., Chen, F., Fu, Q., Dai, A., et al. (2017). Dryland climate change: Recent progress and challenges. *Reviews of Geophysics*, 55(3), 719–778. <https://doi.org/10.1002/2016RG000550>
- Huang, M., Piao, S., Ciais, P., Peñuelas, J., Wang, X., Keenan, T. F., et al. (2019). Air temperature optima of vegetation productivity across global biomes. *Nature Ecology & Evolution*, 3(5), 772–779. <https://doi.org/10.1038/s41559-019-0838-x>
- Huang, X., Xiao, J., Wang, X., & Ma, M. (2021). Improving the global MODIS GPP model by optimizing parameters with FLUXNET data. *Agricultural and Forest Meteorology*, 300, 108314. <https://doi.org/10.1016/j.agrformet.2020.108314>
- Hurst, H. E. (1951). Long-term storage capacity of reservoirs. *Transactions of the American Society of Civil Engineers*, 116(1), 770–799. <https://doi.org/10.1061/TACEAT.0006518>
- Leng, J., Chen, J. M., Li, W., Luo, X., Xu, M., Liu, J., et al. (2024). Global datasets of hourly carbon and water fluxes simulated using a satellite-based process model with dynamic parameterizations. *Earth System Science Data*, 16(3), 1283–1300. <https://doi.org/10.5194/essd-16-1283-2024>
- Li, C., Fu, B., Wang, S., Stringer, L. C., Wang, Y., Li, Z., et al. (2021). Drivers and impacts of changes in China's drylands. *Nature Reviews Earth and Environment*, 2(12), 858–873. <https://doi.org/10.1038/s43017-021-00226-z>
- Li, X., & Xiao, J. (2019). Mapping photosynthesis solely from solar-induced chlorophyll fluorescence: A global, fine-resolution dataset of gross primary production derived from OCO-2. *Remote Sensing*, 11(21), 2563. <https://doi.org/10.3390/rs11212563>
- Li, Y., Huang, J., Ji, M., & Ran, J. (2015). Dryland expansion in northern China from 1948 to 2008. *Advances in Atmospheric Sciences*, 32(6), 870–876. <https://doi.org/10.1007/s00376-014-4106-3>
- Libiseller, C., & Grimvall, A. J. E. (2002). Performance of partial Mann–Kendall tests for trend detection in the presence of covariates. *Environmetrics*, 13(1), 71–84. <https://doi.org/10.1002/env.507>
- Lu, F., Hu, H., Sun, W., Zhu, J., Liu, G., Zhou, W., et al. (2018). Effects of national ecological restoration projects on carbon sequestration in China from 2001 to 2010. *Proceedings of the National Academy of Sciences of the United States of America*, 115(16), 4039–4044. <https://doi.org/10.1073/pnas.1700294115>
- Ma, J., Xiao, X., Miao, R., Li, Y., Chen, B., Zhang, Y., & Zhao, B. (2019). Trends and controls of terrestrial gross primary productivity of China during 2000–2016. *Environmental Research Letters*, 14(8), 084032. <https://doi.org/10.1088/1748-9326/ab31e4>
- Peng, S. (2024a). 1km monthly potential evapotranspiration dataset over China during 1901–2023 [Dataset]. *National Earth System Science Data Center, National Science & Technology Infrastructure of China*. <https://doi.org/10.11866/db.loess.2021.001>
- Peng, S. (2024b). 1km monthly average temperature dataset over China during 1901–2023 [Dataset]. *National Earth System Science Data Center, National Science & Technology Infrastructure of China*. <https://doi.org/10.12041/geodata.164304785536614.ver1.db>
- Peng, S. (2024c). 1km monthly precipitation dataset over China during 1901–2023 [Dataset]. *National Earth System Science Data Center, National Science & Technology Infrastructure of China*. <https://doi.org/10.12041/geodata.192891852410344.ver1.db>
- Peng, S., Ding, Y., Liu, W., & Li, Z. (2019). 1 km monthly temperature and precipitation dataset for China from 1901 to 2017. *Earth System Science Data*, 11(4), 1931–1946. <https://doi.org/10.5194/essd-11-1931-2019>
- Piao, S., Wang, X., Park, T., Chen, C., Lian, X., He, Y., et al. (2020). Characteristics, drivers and feedbacks of global greening. *Nature Reviews Earth and Environment*, 1(1), 14–27. <https://doi.org/10.1038/s43017-019-0001-x>

- Preisendorfer, R. W., & Mobley, C. D. (1988). *Principal component analysis in meteorology and oceanography*. Elsevier.
- Ren, Y., Wang, H., Yang, K., Li, W., Hu, Z., Ma, Y., & Qiao, S. (2024). Vegetation productivity slowdown on the Tibetan Plateau around the late 1990s. *Geophysical Research Letters*, *51*(4). <https://doi.org/10.1029/2023GL103865>
- Running, S., Mu, Q., & Zhao, M. (2015). MOD17A2H MODIS/terra gross primary productivity 8-day L4 global 500m SIN grid V006 [Dataset]. NASA LP DAAC. <https://doi.org/10.5067/MODIS/MOD17A2H.006>
- Sen, P. K. (1968). Estimates of the regression coefficient based on Kendall's tau. *Journal of the American Statistical Association*, *63*(324), 1379–1389. <https://doi.org/10.1080/01621459.1968.10480934>
- Theil, H. (1992). A rank-invariant method of linear and polynomial regression analysis. In B. Raj & J. Koerts (Eds.), *Henri theil's contributions to economics and econometrics. Advanced studies in theoretical and applied econometrics* (Vol. 23, pp. 345–381). Springer. https://doi.org/10.1007/978-94-011-2546-8_20
- Verma, M., Friedl, M. A., Richardson, A. D., Kiely, G., Cescatti, A., Law, B. E., et al. (2014). Remote sensing of annual terrestrial gross primary productivity from MODIS: An assessment using the FLUXNET La Thuile data set. *Biogeosciences*, *11*(8), 2185–2200. <https://doi.org/10.5194/bg-11-2185-2014>
- Wang, A., Zhang, M., Chen, E., Zhang, C., & Han, Y. (2024). Impact of seasonal global land surface temperature (LST) change on gross primary production (GPP) in the early 21st century. *Sustainable Cities and Society*, *110*, 105572. <https://doi.org/10.1016/j.scs.2024.105572>
- Wang, L., Jiao, W., MacBean, N., Rulli, M. C., Manzoni, S., Vico, G., & D'Odorico, P. (2022). Dryland productivity under a changing climate. *Nature Climate Change*, *12*(11), 981–994. <https://doi.org/10.1038/s41558-022-01499-y>
- Wang, X., Ge, Q., Geng, X., Wang, Z., Gao, L., Bryan, B. A., et al. (2023). Unintended consequences of combating desertification in China. *Nature Communications*, *14*(1), 1139. <https://doi.org/10.1038/s41467-023-36835-z>
- Wei, X., Ye, Y., Zhang, Q., & Fang, X. (2016). Reconstruction of cropland change over the past 300 years in the Jing-Jin-Ji area, China. *Regional Environmental Change*, *16*(7), 2097–2109. <https://doi.org/10.1007/s10113-016-0933-3>
- Wu, B., Fu, Z., Fu, B., Yan, C., Zeng, H., & Zhao, W. (2024). Dynamics of land cover changes and driving forces in China's drylands since the 1970s. *Land Use Policy*, *140*, 107097. <https://doi.org/10.1016/j.landusepol.2024.107097>
- Xiao, Z., Liang, S., Wang, J., Xiang, Y., Zhao, X., & Song, J. (2016). Long-time-series global land surface satellite leaf area index product derived from MODIS and AVHRR surface reflectance. *IEEE Transactions on Geoscience and Remote Sensing*, *54*(9), 5301–5318. <https://doi.org/10.1109/TGRS.2016.2560522>
- Xie, S., Mo, X., Hu, S., & Liu, S. (2020). Contributions of climate change, elevated atmospheric CO₂ and human activities to ET and GPP trends in the Three-North Region of China. *Agricultural and Forest Meteorology*, *295*, 108183. <https://doi.org/10.1016/j.agrformet.2020.108183>
- Xie, X., Li, A., Jin, H., Tan, J., Wang, C., Lei, G., et al. (2019). Assessment of five satellite-derived LAI datasets for GPP estimations through ecosystem models. *Science of the Total Environment*, *690*, 1120–1130. <https://doi.org/10.1016/j.scitotenv.2019.06.516>
- Xu, L., Gao, G., Wang, X., & Fu, B. (2023). Distinguishing the effects of climate change and vegetation greening on soil moisture variability along aridity gradient in the drylands of northern China. *Agricultural and Forest Meteorology*, *343*, 109786. <https://doi.org/10.1016/j.agrformet.2023.109786>
- Yan, G., Hu, R., Luo, J., Weiss, M., Jiang, H., Mu, X., et al. (2019). Review of indirect optical measurements of leaf area index: Recent advances, challenges, and perspectives. *Agricultural and Forest Meteorology*, *265*, 390–411. <https://doi.org/10.1016/j.agrformet.2018.11.033>
- Yao, J., Liu, H., Huang, J., Gao, Z., Wang, G., Li, D., et al. (2020). Accelerated dryland expansion regulates future variability in dryland gross primary production. *Nature Communications*, *11*(1), 1665. <https://doi.org/10.1038/s41467-020-15515-2>
- Yu, G., Zhu, X., Fu, Y., He, H., Wang, Q., Wen, X., et al. (2013). Spatial patterns and climate drivers of carbon fluxes in terrestrial ecosystems of China. *Global Change Biology*, *19*(3), 798–810. <https://doi.org/10.1111/gcb.12079>
- Zhang, X., Liang, S., Zhou, G., Wu, H., & Zhao, X. (2014). Generating Global Land Surface Satellite incident shortwave radiation and photosynthetically active radiation products from multiple satellite data. *Remote Sensing of Environment*, *152*, 318–332. <https://doi.org/10.1016/j.rse.2014.07.003>
- Zhang, Y., Desai, A. R., Xiao, J., & Hartemink, A. E. (2023). Deeper topsoils enhance ecosystem productivity and climate resilience in arid regions, but not in humid regions. *Global Change Biology*, *29*(23), 6794–6811. <https://doi.org/10.1111/gcb.16944>
- Zhou, L., Chen, H., Hua, W., Dai, Y., & Wei, N. (2016). Mechanisms for stronger warming over drier ecoregions observed since 1979. *Climate Dynamics*, *47*(9–10), 2955–2974. <https://doi.org/10.1007/s00382-016-3007-9>